Journal of
Materials Chemistry A

Rational design and fabrication of core-shell nanoparticles through one-step/pot strategy

Journal:	Journal of Materials Chemistry A
Manuscript ID	TA-REV-11-2015-009607.R1
Article Type:	Review Article
Date Submitted by the Author:	15-Jan-2016
Complete List of Authors:	Liu, Rui; Tongji University Priestley, Rodney; Princeton University, Chemical and Biological Engineering

SCHOLARONE™
Manuscripts

Journal Name

ARTICLE

Rational design and fabrication of core-shell nanoparticles through one-step/pot strategy

Rui Liu[a]* and Rodney D. Priestley[bc]*

Core-shell nanoparticles (NPs) have emerged as a type of important nanomaterials for various applications. The challenge in the preparation of core-shell NPs is to find a simple, cost-effective and less time-consuming strategy with minimum environmental impact. The consolidation of multiple preparation steps into one step represents a new green synthesis pathway in chemistry and materials science. In this review, we provide an overview of the recent developments in the fabrication of core-shell NPs through one-step/pot methodologies. A variety of one-step/pot preparation methods are presented, discussed and compared, followed by the summary and outlook of this emerging area.

1. Introduction

The rapid development of nanotechnology over the past few decades has lead to the emergence of core-shell nanoparticles (NPs) as a new type of important functional material.[1] Core-shell NPs with different functional compositions are being widely investigated because of their potential applications in many fields, such as electronics, biomedical, pharmaceutical, optics, and catalysis.[2-5] The coating shell on the precious core materials would not only increase the functionality, stability and dispersibility, but also reduce the consumption of precious materials. Both from technological and economic points of view, core-shell NPs represent a type of important materials in energy, environment and sustainability. The core-shell type NPs can be broadly defined as comprising a core (inner material) and a shell (outer layer material). The core may be a single sphere (Fig.1A) or aggregation of several small spheres[6] (Fig.1B). It is also possible to have a small sphere entrapped inside a hollow shell, a rattle-like or yolk-shell structure[7] (Fig.1C). Beside continuous layer, the shell structure can also be an attachment of smaller spheres onto a bigger core sphere[8] (Fig.1D). Complex core-shell structures are made possible with multiple shells[9] (Fig.1E) or may also be represented as the combination of other basic structures[10] (Fig.1F).

The core and the shell can be different materials or the same materials with different structures. In general, core-shell nanostructures can be divided into several classes depending
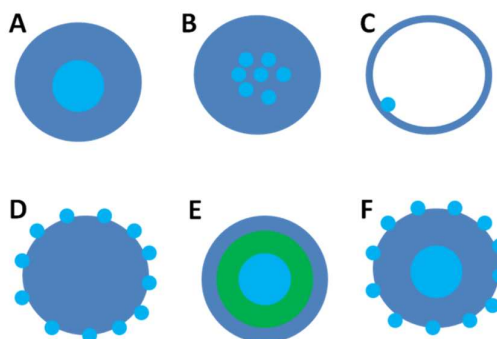

Fig. 1 Schematic representation of different types of core–shell particles

on the compositions, including inorganic/inorganic[11], inorganic/organic[12], organic/inorganic[13] and organic/organic[14] type. The properties arising from either core or shell materials can be modified by changing the constituting materials or the core/shell ratio. The size of the core particle, the shell thickness and the porosity in the core or the shell can be tuned to meet different requirements. Besides its own functionality, core-shell NPs can also serve as a structured template for the preparation of hollow particles after removing the core either by dissolution or calcination.[15-17]

Traditional synthesis of core-shell NPs is through a two-step or multiple-step process. The core particles are pre-synthesized and depending on the interaction between the core and the shell, the shell is then formed on the core particle *via* different methods. Layer-by-layer coating utilizes the electrostatic interactions between the positively charged and negatively charged species to assemble multiple layers together.[18] The polymerization of shells on pre-formed cores represents another common technology for a large percentage of core-shell particles.[19,20] One important challenge, often faced by synthetic chemists and materials scientists, is the development of robust, low-cost and environmentally benign

a. School of Materials Science and Engineering, Institute of Advanced Study, Tongji University, Shanghai, 201804, China ruiliu@tongji.edu.cn
b. Department of Chemical and Biological Engineering, Princeton University, Princeton, New Jersey, 08544, USA rpriestl@princeton.edu
c. Princeton Institute for the Science and Technology of Materials, Princeton University, Princeton, NJ, 08544 USA

core-shell nanomaterials through a facile, green and efficient methodology. Great progress has been made and many examples have been reported in the synergistic preparation of core-shell NPs through a one-step/pot strategy during the past decade. Rational selection of precursor is prerequisite for all the precursors should have ability to form core or shell materials under the same reaction condition. Design of the interaction between the core and the shell is another important factor to control core grow and shell coating. In this review, we provide a focused summary of recent progress in the one-step/pot construction of core-shell nanostructures. Due to the large amount of reports on this aspect, we have only focused on molecular design and experimental preparation for core-shell NPs. The structure-property relationships and the applications of the synthesized materials have been not included here as they have been extensively discussed in other reviews.[1-5,21-23]

2. Simultaneous Oxidation-Reduction

2. 1 Co-reduction

In situ co-reduction and seeding-growth was developed for the one-step synthesis of core-shell bimetallic NPs. The difference in reduction potentials of different metal ions is key factor, by which the metal ions with higher reduction potential are reduced first and then serve as the *in situ* seeds for the successive reduction of shell metal ions. Xu and co-workers prepared Au@Co core-shell NPs using ammonia-borane to simultaneously reduce Au^{3+} and Co^{2+} precursors based on the difference in reduction potentials of the two soluble metal salts ($E^{o}_{Co2+/Co}$= -0.28 eV *vs* SHE; $E^{o}_{Au3+/Au}$= +0.93 eV *vs* SHE).[24] The synthesis progress can be visibly monitored by the evolution of solution colour, changing from light-pink to orange-red, then to black (Fig. 2). They found that a suitable reductant is essential because strong reductants inevitably lead to the formation of binary alloys, while reducing agents are too weak and cannot effectively reduce the metal precursors. The same group also prepared Au@Co@Fe core-shell-shell NPs through *in situ* co-reduction of $HAuCl_4$, $CoCl_2$ and $FeCl_3$.[25]

Core-alloy shell NPs can also be one-step synthesized through suitable selection of metal ions and reductants. Han and co-workers reported a one-step co-reduction method for the preparation of trimetallic Au@PdPt core-shell NPs with a well-defined octahedral Au
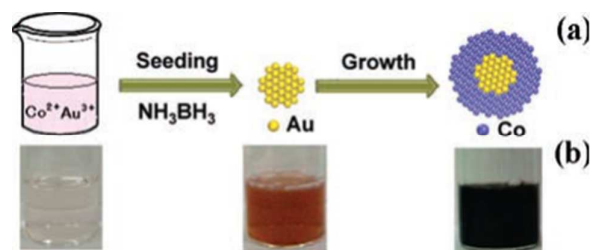

Fig . 2 (a) Schematic illustration, (b) color evolution in the formation process of Au@Co core-shell NPs via a one-step co-reduction method. Reproduced with permission from ref. 24. Copyright 2010, American Chemical Society
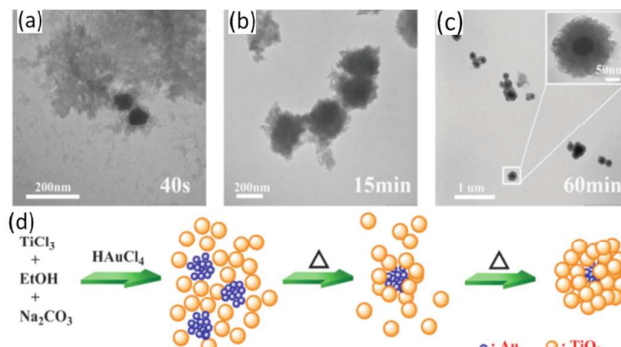

Fig . 3 TEM images of samples collected from the reaction system after (a) 40 s, (b) 15 min, (c) 60 min, and (d) schematic illustration of the formation of Au@TiO₂ core-shell composites. Reproduced with permission from ref. 42. Copyright 2014, Wiley-VCH Verlag GmbH & Co. KGaA.

core and a highly crystalline dendritic PdPt alloy shell.[26] The simultaneous reduction of multiple metal precursors, namely, a $HAuCl_4$-K_2PdCl_4-K_2PtCl_6 mixture, was performed with dual reducing agents, ascorbic acid and hydrazine. The one-step co-reduction gave a fine control over the nucleation and growth kinetics, resulting in the formation of Au@PdPt. Typical core-shell NPs, precursors, reductants and particle morphology through one-step co-reduction are listed in Table 1.

2.2 Redox reaction

In situ redox reactions has been demonstrated in the integration of different metals and metal oxides to fabricate core-shell hybrid materials. Synthesis of Au@TiO₂ involves redox reactions between Ti^{3+} and Au^{3+} ions in the presence of ethanol and Na_2CO_3.[42] Au^{3+} ions were immediately reduced by Ti precursors and nucleated rapidly to form clusters and meanwhile, Ti^{3+} was oxidized by the Au^{3+} ions, hydrolyzed, and assembled on the surface of Au NPs, leading to the formation of Au@TiO₂ (Fig. 3). Ag@CeO₂[43,44] and Pt@CeO₂[45] core-shell composites have been synthesized using the redox reactions between oxidative noble metal ions and reductive cerium(III) nitrate. The materials exhibited excellent catalytic properties in the oxidation of CO and chemoselective reduction reactions.[46]

Simultaneous oxidative polymerization of monomer and growth of metal nanostructures were confirmed in the fabrication of metal-polymer core-shell NPs. The adjustable conductivity, ease of oxidation, and good environmental stability endow conducting polymers (e.g., polyaniline, PAN and polypyrrole, PPY) great potential in the construction of shell layers.[47-55] Ag@PPY nanosnakes have been prepared by polymerization of pyrrole in the presence of Ag₂O under hydrothermal condition.[47,48] Au@PPY was obtained by simply mixing pyrrole monomer with $HAuCl_4$ in an aqueous solution, where the $HAuCl_4$ is spontaneously reduced by pyrrole to form gold dendrite while the pyrrole is simultaneously oxidized to grow polypyrrole thin film and deposit on Au NPs.[49] Novel polymers are being explored and employed in the redox-controlled fabrication of core-shell NPs. Polydopamine (PDA) has received significant attention due to its unique coating quality and reducing ability.[56] One-step synthesis of core–shell Ag@PDA structures was demonstrated *via* simple oxidative polymerization of dopamine monomers by Ag^+ ion.[57] The DA serves as a reducing agent and a monomer, while Ag^+ ions as

Table 1 One-step co-reduction preparation of core-shell NPs

Core/Shell	Precursor	Reductant	Particle morphology	Ref.
Au/Co	$HAuCl_4/CoCl_2$	NH_3BH_3	roughly spherical	24
Au/Co/Fe	$HAuCl_4/CoCl_2/FeCl_3$	NH_3BH_3	roughly spherical	25
Au/Pd	$HAuCl_4/K_2PdCl_4$	cetyltrimethylammonium chloride	nanooctahedron	27
	$HAuCl_4/PdCl_2$	bayberry tannin	spherical or cubic	28
	$HAuCl_4/Na_2PdCl_4$	reduced graphene oxide	nanocluster	29
	$HAuCl_4/H_2PdCl_4$	polyvinylpyrrolidone	near Spherical	30
	$HAuCl_4/PdCl_2$	ethylene glycol(EG)	irregular	31
Au/Pt	$HAuCl_4/H_2PtCl_6$	polyethylene glycol(PEG)	spherical	32
Au/PdPt	$HAuCl_4/$ K_2PdCl_4/K_2PtCl_6	ascorbic acid and hydrazine	nanooctahedron	26
Au/Pd/Pt	$HAuCl_4/K_2PtCl_4/ Na_2PdCl_4$	ascorbic acid	dendritic	33
Ag/Ni	$AgNO_3 /Ni(NO_3)_2$	bayberry tannin	spherical	34
	$AgNO_3 /Ni(NO_3)_2$	$NaBH_4$	spherical	35
Au/Ag	$HAuCl_4/AgNO_3$	EG and PEG	irregular	36
Ag/Au	$AgClO_4 /HAuCl_4$	$NaBH_4$	spherical	37
Pd/Pt	$K_2PtCl_4 /PdCl_2$	ascorbic acid	spherical	38
	K_2PdCl_4/K_2PtCl_4	ascorbic acid	cube cores/dendritic shells	39
	$PdCl_2/ K_2PtCl_4,$	ascorbic acid	star-like	40
Cu/FeNi	$CuCl_2/FeSO_4/NiCl_2$	$NH_3BH_3,$	roughly spherical	41

the oxidant to trigger the DA polymerization and the source of the metallic NPs. Fe$_3$O$_4$@PDA NPs were synthesized though one-step electrochemical process.[58] Magnetite NPs were produced by electro-oxidation of iron in an aqueous medium in the presence of dopamine. The oxidative conditions and alkaline pH involved in the synthesis favored the self-polymerization of dopamine that adheres at the surface of the magnetic NPs in a simultaneous process.

2.3 Hydrothermal reduction-carbonization

The hydrothermal carbonization (HTC) process can generate a variety of core-carbon shell materials with attractive properties. Biomass (e.g., glucose, sucrose, starch and lactose) is widely used and converted into interesting carbon nanostructures during HTC coating process.[59-68] Li *et al.* reported a series of metals or metal oxides encapsulated in carbon by in situ hydrothermal reduction of noble-metal ions with glucose.[69-71] Zong *et al.* prepared Fe$_x$O$_y$@C core-shell catalysts from iron nitrate and glucose by a one-pot hydrothermal method (Fig. 4a and b).[72] During the HTC process, iron nitrate catalyzes the dehydration of glucose at

the initial stage of the synthesis, leading to small carbonaceous colloids with a low degree of polymerization. Meanwhile, iron nitrate is transformed to FeOOH under the hydrothermal conditions and further reduced to Fe$_x$O$_y$ by hydrogen released from the carbonization process. The Fe$_x$O$_y$ NPs then combine with small carbonaceous colloids through Coulombic interactions and are further homogeneously distributed in the carbonaceous spheres.

Lou and co-workers directly carbonized a capping agent (e.g., polyvinylpyrrolidone, PVP) during HTC for the preparation of MoO$_2$@C nanospheres (Fig.4c and d).[73] At first, MoO$_2$ nanocrystals prepared by the reduction of ammonium heptamolybdate tetrahydrate with ethylene glycol. Excess amount of PVP is introduced as the capping agent to prevent overgrowth of the primary MoO$_2$ nanocrystals, as well as over-agglomeration of the assembled MoO$_2$ nanospheres. After simple annealing under an inert atmosphere, a thin carbon layer is simultaneously generated on the surface of the nanospheres from carbonization of absorbed organic residues, resulting in the formation of MoO$_2$@C nanospheres.
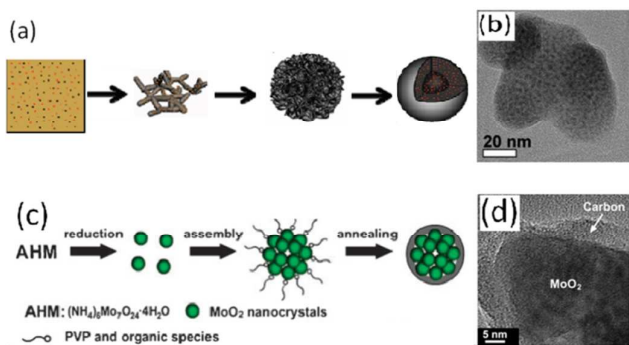
3. One-step Stöber synthesis

3.1 Stöber silica shell

The stöber method is the most established and facile approach for the preparation of silica colloidal spheres and silica coated composites through the hydrolysis and condensation of a silica source, such as tetraethylorthosilicate (TEOS), in basic water/alcohol solutions.[74] By optional selection of metal precursors, reducing agents, and surfactants, a series of metal-silica core-shell nanomaterials, such as Au@SiO$_2$[75-77], Ag@SiO$_2$[78], Fe@SiO$_2$[79]and Cu@SiO$_2$[80], through a simple one-pot stöber method have been successfully prepared. For example, Zhao and co-workers reported one-pot synthesis of uniform core-shell nanospheres with a Au nanoparticle core and a mesoporous silica shell by using HAuCl$_4$ as a precursor, formaldehyde as a reducing agent, cetyltrimethylammonium bromide (CTAB) as the stabilizer
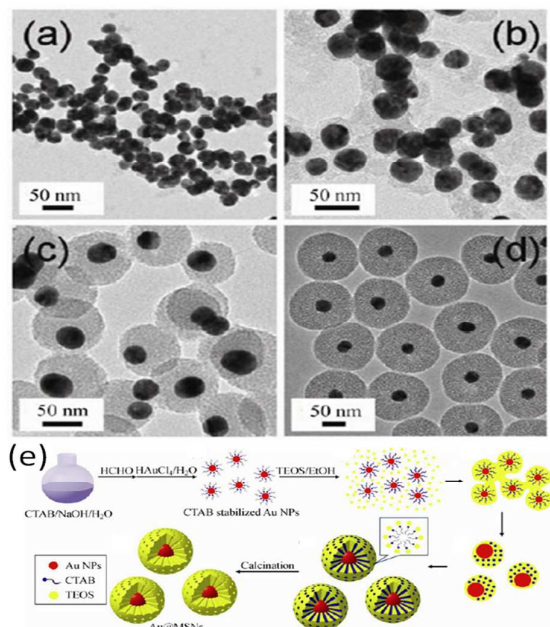

Fig . 4 (a) Schematics of one-pot formation and (b) TEM of Fe$_x$O$_y$@C NPs.[72] (c) Schematics of one-pot formation and (d) TEM of MoO$_2$@C nanospheres.[73] Adapted with permission from ref. 72. Copyright 2010, American Chemical Society and ref. 73. Copyright 2010, The Royal Society of Chemistry.

and

Fig . 5 TEM images of samples collected from the reaction system (a) 10 min after the addition of HCHO and HAuCl$_4$, (b) 5 min, (c) 15 min, and (d) 50 min after the addition of TEOS, and (e) schematic illustration of the formation of Au@SiO$_2$ core-shell composite. Adapted with permission from ref. 75 Copyrights 2010, Springer

template, TEOS as the silica source, and sodium hydroxide as a basic catalyst.[75] TEM images of the samples obtained after different reaction times show that the formation process involves the growth of a gold core followed by coating with a mesoporous silica shell (Fig. 5a-d). As a result, the one-step synchronous process shown in Fig. 5e combines several steps into one, including the reduction of HAuCl$_4$, assembly of surfactant-stabilized Au nanocrystals and silica-surfactant micelles, transfer and aggregation of Au nanocrystals to form a Au core in condensed silica mesostructures. He and co-workers developed a facile one-pot stöber method for the fabrication of Au NPs encapsulated inside hollow silica.[81] As shown in Fig.6, poly(acrylic acid) (PAA) was added into the one-pot process, where PAA played a dual role during the fabrication, both as a core template of the hollow silica sphere and as a captor of Au NPs through coordination interactions between the COO$^-$ groups on the polyanionic chains and the empty orbital of the Au atom. The amount of Au loading in one hollow silica sphere was easily regulated by varying the volume of the HAuCl$_4$ solution added. Other hydrolysis and condensation processes have also been applied in the fabrication of core-oxide shell nanostructure. For example, Ag@ZnO NPs were prepared by the one-pot feeding of silver nitrate and zinc acetate in *N,N*-dimethylformamide (DMF), where the solvent simultaneously behaves as a reducing agent for Ag$^+$ ions and provides the basic medium for zinc acetate hydrolysis at room temperature.[82] Similarly, Ag@TiO$_2$ NPs were one-pot prepared by simultaneously feeding silver nitrate and Ti(OC$_4$H$_9$)$_4$ in DMF.[83]

Metal oxide-silica core-shell, namely, Fe$_3$O$_4$@SiO$_2$ can be prepared through one-pot stöber method by combining the Massart method for magnetite nanoparticles and the mesoporous silica.[84] In addition, Zhang *et al.* reported one-pot synthesis of SiO$_2$-SiO$_2$ core–shell, which contained a solid microsphere core (about 5.5 μm)
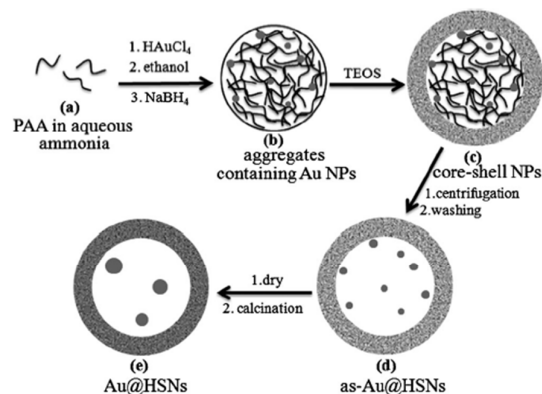

Fig . 6 Schematic illustration of the formation of Au@hollow SiO$_2$ core-shell composite. . Reproduced with permission from ref. 81. Copyright 2012, Wiley-VCH Verlag GmbH & Co. KGaA

with coated nanospheres of 200 nm, from one single precursor 3-mercaptopropyltrimethoxysilane under stöber condition.[85,86] SEM images at different reaction times show that the structure evolution consisted the initial formed microspheres, followed by the growth of new silica nanospheres on the microsphere surface. The application of SiO$_2$@SiO$_2$ particles in chromatography showed fast separation of protein mixtures at low back pressure.

3.2 Stöber polymer shell

A major breakthrough in the development of core-shell fabrication was achieved in 2011 by extending the stöber method for the preparation of resorcinol–formaldehyde (RF) resin spheres.[87] Due to its ability to form a coordinated covalently bonded framework during polymerization similar to silica, the stöber method was successfully confirmed by preparation of monodisperse RF spheres with tunable particle sizes.[87] The extension of the stöber method for polymer synthesis opens the pathway for synthetic strategies in the preparation of not only RF based polymer spheres and derived carbon spheres, but also for the development of one-step synthesized core-RF shell NPs. A one-step method was first reported to produce uniform SiO$_2$@RF polymer spheres with a core-shell structure by combining the synthesis processes of silica and resorcinol-formaldehyde under stöber conditions.[88] Although both occur under similar reaction conditions (i.e., reaction medium, temperature and catalyst), the polymerization reactions of silica and resorcinol-formaldehyde occurring at different time scales was
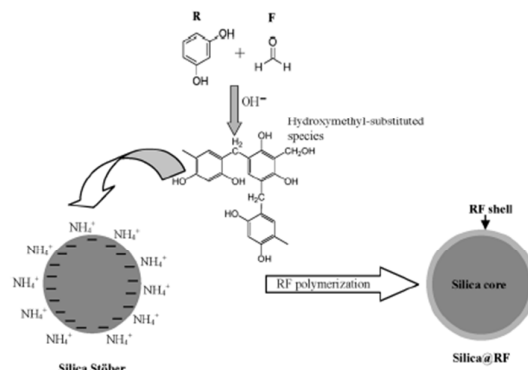

Fig . 7 Schematic illustration of the formation of SiO$_2$@RF composites. Reproduced with permission from ref. 88. Copyright 2012, The Royal Society of Chemistry.
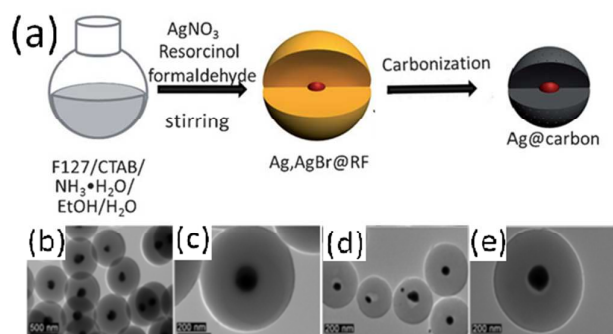
Fig . 8 (a) Synthesis procedures of Ag,AgBr@RF and Ag@carbon core-shell nanospheres, and TEM images of (b,c) Ag,AgBr@RF core-shell spheres and C,D) Ag@carbon core-shell spheres. Adapted with permission from ref. 89. Copyright 2013, Wiley-VCH Verlag GmbH & Co. KGaA.

key to the formation of silica@RF polymer core-shell nanoparticles. The synthesis time of stöber silica particles is 1 hour at 30°C while the formation of RF particles occurs slower and requires a reaction time greater than 24 h. The electrostatic interaction between the RF oligomer and the early staged formed silica particles would direct the condensation of RF around the silica particles. (Fig. 7)

Qiao and co-workers synthesized Ag,AgBr@RF core-shell NPs by a one-pot stöber method involving simultaneous reduction of AgNO$_3$ and polymerization of RF resins in the presence of ammonia, with CTAB and the triblock polymer F127 as costabilizers.[89] As shown in Fig. 8, CTAB first forms micelles with F127 to stabilize AgBr-core NPs. Then, the RF monomers aggregate on the micelles to form emulsion droplets; meanwhile, Ag$^+$ is reduced to Ag^0 by formaldehyde to form Ag/AgBr-composite cores. Simultaneously, Ag/AgBr-composite cores are encapsulated by RF polymer. Formaldehyde plays a dual

role in the formation of the core-shell structure: it reduces Ag$^+$ to Ag^0 in situ and crosslinks with resorcinol to form the precursor RF polymer. Further annealing of the Ag,AgBr@RF core-shell particles to carbonize the RF shell results in unique core-shell-structured Ag@carbon spheres with 20% shrinkage in size. The same one-pot strategy was also successfully confirmed in the preparation of

Te@RF nanowires starting from sodium tellurite.[90]

3.3 Stöber double shells

Uniform core-shell-shell (CSS) NPs with different functional compositions are another important type of core-shell nanomaterials. One application of the core-shell-shell NP is their use as a template to develop various new nanostructures. Among them, the rattle-type or yolk–shell nanostructure is a novel and promising nanostructure, in which a movable core is encapsulated inside a polymer or inorganic shell.[91-93] Usually, the synthesis of core-multiple shell NPs requires multiple coating processes. Priestley and co-workers reported a one-step strategy to simplify the multiple coating process.[94] As illustrated in Fig. 9a, the Au-Silica-RF polymer CSS nanostructures is simply obtained by feeding Au colloids, TEOS, resorcinol, and formaldehyde in a mixture of alcohol and aqueous ammonia. The different reaction kinetics is key to the successful formation of the CSS nanostructures. A series of TEM images at the different reaction times indicated that Au@SiO$_2$ core-shells with ~150 nm particle sizes were formed within 1h while no obvious RF polymer layer was observed even after 12h of reaction time (Fig. 9b-d). A thin 5 nm RF outer layer was formed after 24h (Fig. 9e). The hydrothermal treatment at 100 ^{o}C for another 24h grew the RF layer up to 18 nm, as indicated in Fig. 9f. The approach combines the fast coating of metal NPs by stöber silica with the slow polymerization of stöber RF polymer and provides a route to form CSS nanostructures, which can be further transformed into Au@C yolk-shell NPs (Fig. 9g). Metal oxide-SiO$_2$-RF core-shell-shell NPs were also prepared by one-step stöber method when feeding pre-synthesized metal oxide NPs into the initial reaction solution.[95]

Priestley and coworkers further simplified the coating process by starting with the metal salts instead of pre-synthesized metal nanocrystals in the preparation of CSS nanostructures. As illustrated in Fig.10a, the synthesis can be undertaken by feeding AgNO$_3$, TEOS, resorcinol, and formaldehyde with CTAB, in a mixture of alcohol and aqueous ammonia.[96] TEM images show that the
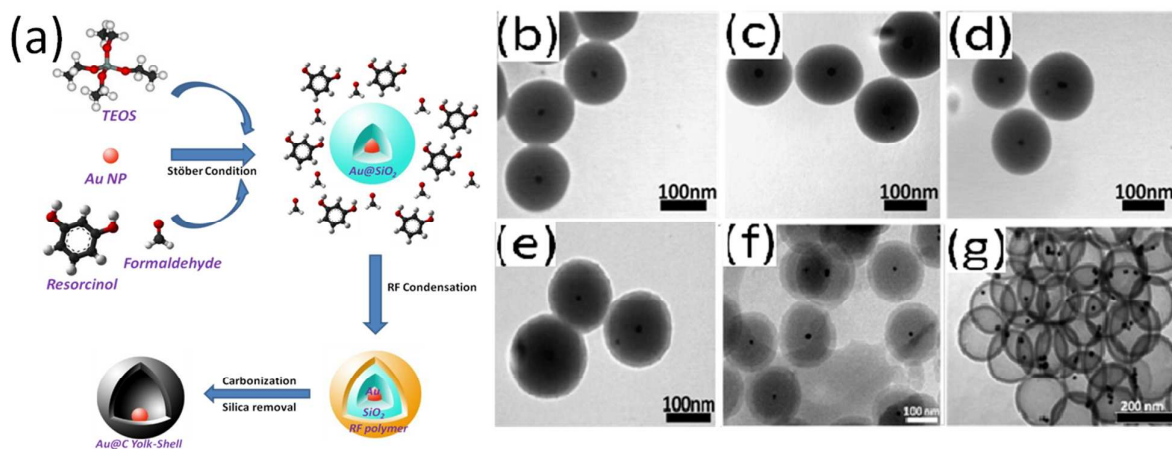

Fig . 9 (a)schematic illustration of one-step synthesis of Au@SiO$_2$@RF CSS and conversion into Au@carbon yolk-shell nanospheres, and TEM images of Au@SiO$_2$@RF CSS obtained with different reaction times (b)1h, (c)6h, (d)12h, (e)24h, (f)48h, and (g) TEM images of Au@C yolk-shell NPs. Adapted with permission from ref. 94. Copyright 2014, The Royal Society of Chemistry.
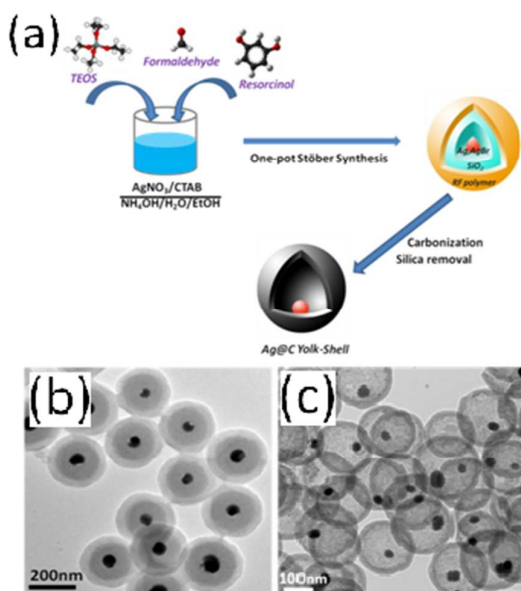
Fig. 10 (a)schematic illustration of one-step synthesis of Ag,AgBr@SiO$_2$@RF CSS and conversion into Ag@carbon yolk-shell nanospheres, and TEM images of (b) Ag,AgBr@SiO$_2$@RF and (c) Ag@C yolk-shell. Adapted with permission from ref. 96. Copyright 2014, The Royal Society of Chemistry.

formation process involves the growth of a Ag/AgBr core followed by coating with a porous silica shell and subsequently a RF polymer outer layer. During the process, CTAB stabilized AgBr-cores are covered by the silica layer and partially reduced to Ag by formaldehyde to form an Ag,AgBr-silica core-shell. After subsequent addition of resorcinol for another 6 h, the Ag,AgBr core was covered by a denser layer of silica with ~170nm particle size while no obvious RF polymer layer was observed. Only after 24 h of reaction time was a 5 nm thick outer RF layer observed. After hydrothermal treatment at 100 ^{o}C for 24 h, the RF layer thickness grew to a thickness of 35 nm and the core-shell-shell Ag,AgBr-silica-RF were obtained and carbonized into Ag@C nanoparticles (Fig. 10b and c). The whole process combines the simultaneous Ag$^+$ reduction by formaldehyde, the fast coating of Ag/AgBr NPs by stöber silica with

the slow polymerization of stöber RF polymer to provide a one-pot route to simplify the fabrication process of CSS nanostructures, which usually entails multiple steps and previously synthesized metal NPs.

4. Self-assembly

4.1 Co-precipitation

Encapsulation of preformed inorganic NPs into polymer micelles can be performed through one-step assembly of NPs and amphiphilic block copolymer in selective solvent to obtain NP@Polymer core-shell nanostructures. Taton and co-workers used a co-precipitation approach and prepared core-shell NPs based on amphiphilic polystyrene–poly(acrylic acid) (PS–PAA) and hydrophobic NPs.[97-99] Taking Fe$_2$O$_3$@Polymer[97] as a example (Fig.11a), PS–PAA and oleic acid-stabilized Fe$_2$O$_3$ were dissolved in a good solvent mixture of DMF and THF. Selective anti-solvent (e.g., water) simultaneously desolvated the NPs and the hydrophobic polymer block (PS), leading to the aggregation of the NPs with the hydrophobic block protected by the hydrophilic segment (PAA). The average number of encapsulated particles per micelle could be controlled by varying the relative starting concentrations of NPs and polymer. Increasing numbers of NPs were incorporated into each micelle with increasing particle concentration (Fig. 11a). The hydrophilic PAA shell could be further crosslinked to avoid dissociation as well as to create a stable vessel that could undergo reversible expansion and contraction. Wooley *et al.* applied the one-step co-precipitated magnetic shell cross-linked NPs in a contaminated aqueous environment, which resulted in the successful removal of the hydrophobic contaminants at a ratio of 10 mg of oil per 1 mg of hybrid NP.[100] On the other hand, the arrangement/location of NPs as well as the polymer morphology can be controlled during the one-step co-precipitation process by changing the initial solvent composition, polymer lengths, weight fractions and surface ligand of NPs.[101-103] Park *et al*. controlled the location of NPs in colloidal block-copolymer assemblies by using NPs modified with mixed surface ligands, dodecanethiol (DT) and mercaptoundecanol (MUL).[101] The AuNPs immobilized with 100% DT segregated into the PS core of polymer micelles due to the favorable enthalphic interactions between the hydrophobic NPs and the PS block as well as the attractive interactions between AuNPs (Fig. 11b). As the fraction of MUL increased to 25% or 33%,
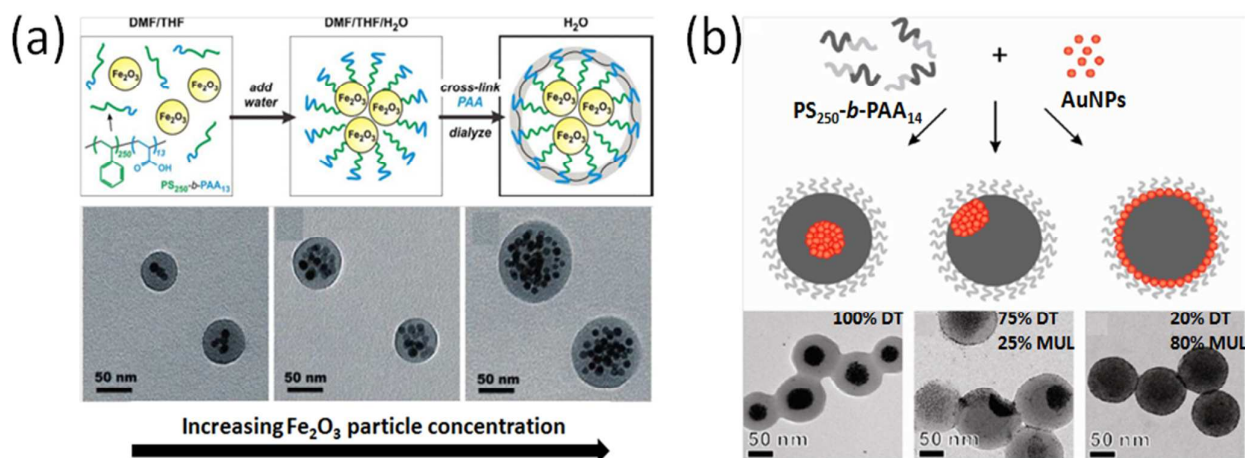

Fig . 11 Schematic illustration and TEM of (a) co-precipitation of PS-*b*-PAA and Fe$_2$O$_3$ NPs, and (b) PS-*b*-PAA and AuNPs with varying surface ligands Adapted with permissions from ref. 127 and 128. Copyrights 2005 and 2013, American Chemical Society, respectively.
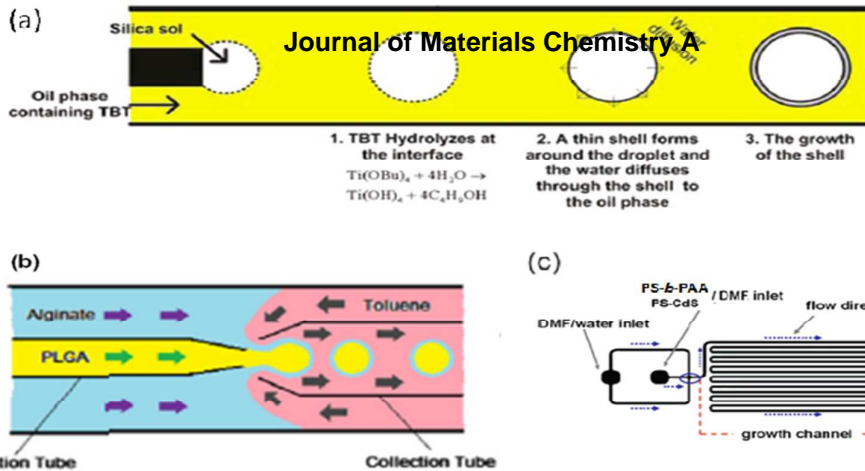
Fig. 12 The mechanism of the core-shell microsphere generation by microfluidic process: (a) SiO$_2$@TiO$_2$, (b) PLGA@alginate and (c) CdS@PS-*b*-PAA. Reproduced with permission from ref.108. Copyright 2011, American Chemical Society and ref. 109. Copyright 2013, Elservier;. Adapted with permission from ref. 111. Copyright 2008, American Chemical Society

the nanoparticle aggregates moved toward the PS–PAA interface, forming Janus-type particles. A further increase of the MUL over 50% led to AuNPs distributed at the PS–PAA interface.

4.2 Microfluidic

Microfluidics concerns small (from 10^{-9} to 10^{-18} liter) volumes of fluids, using channels with dimensions from tens to hundreds of micrometers. Continuous microfluidic synthesis of organic and inorganic compounds offers a number of advantages in comparison with conventional batch synthesis or continuous synthesis conducted in tubular reactors.[104-107] Typically, microfluidics produce extremely monodisperse emulsions/double emulsions and microspheres with complex morphology and compositions in the preparation of core-shell nanostructures. For example, a silica sol were dispersed into an oil phase containing tetrabutyl titanate *via* a coaxial microfluidic device (Fig. 12a).[108] The titanium alkoxide hydrolyzed at the water-oil interface after the formation of the aqueous droplets. A gel shell containing the titanium hydroxide formed around the droplets, and the SiO$_2$-TiO$_2$ core-shell microspheres were obtained after calcinations. On the other hand, a double emulsion approach is more used in producing core–shell particles *via* the microfluidic approach.[107] The PLGA-alginate core-shell microspheres were fabricated using a capillary microfluidic device for generating an oil-in-water-in-oil double emulsion as a template.[109,110] As shown in Fig. 12b, poly(lactide-co-glycolide) (PLGA)/dichloromethane solution was injected through an inner capillary into a flow of aqueous alginate solution. The resulting oil-in-water emulsion droplets were then dispersed in a flow of toluene. The crosslinking of alginate and removal of solvent dichloromethane produced PLGA-alginate core–shell particles .

Co-precipitation of core-shell NPs can also be realized through a microfluidic approach. The controlled self-assembly of polymer-stabilized quantum dots (QDs) into mesoscale aqueous spherical assemblies was one-step accomplished using microfluidics.[111] The microfluidic device employed here involved combining a stream containing the polystyrene-coated QDs (PS-CdS) and amphiphilic PS-*b*-PAA constituents in DMF with a sheath flow of DMF/water solution, followed by a quench step with pure water (Fig. 12c). In a flow-focusing configuration, self-assembly is initiated by the addition of water to a blended solution of PS-CdS and PS-*b*-PAA stabilizing chains and terminated in a downstream quench step. Farokzhad and co-workers have developed a microfluidic platform to achieve a rapid mixing and precipitation.[112,113] They found that, in contrast to slow mixing, rapid mixing directly results in the formation of homogeneous NPs with relatively narrow size distribution.

4.3 Flash Nanoprecipitation (FNP)

FNP is a rapid self-assembly processing technique used to create NPs of uniform size within 30 nm to 800nm. It is a process in which two high velocity linear jets of fluid, one containing the block copolymer solution and the other containing a non-solvent for the polymer, mix in a small chamber using a multi-inlet vortex or confined impinging jets mixer (Fig. 13).[114-117] The block copolymer solution rapidly mixes with the non-solvent for a few milliseconds to induce self-assembly of the block copolymers into kinetically frozen NPs. The main advantages of FNP are that it is a three-component process (involving only bulk polymer, a solvent, and a non-solvent),
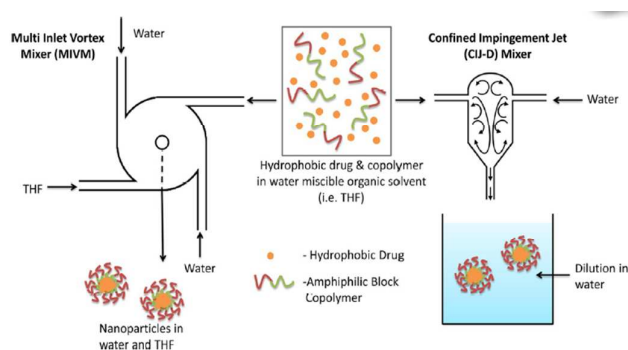

Fig. 13 Schematic diagram of the multi inlet vortex (MIV) mixer and the confined impingement jet (CIJ-D) Reproduced with permission from ref. 117. Copyright 2013, American Chemical Society
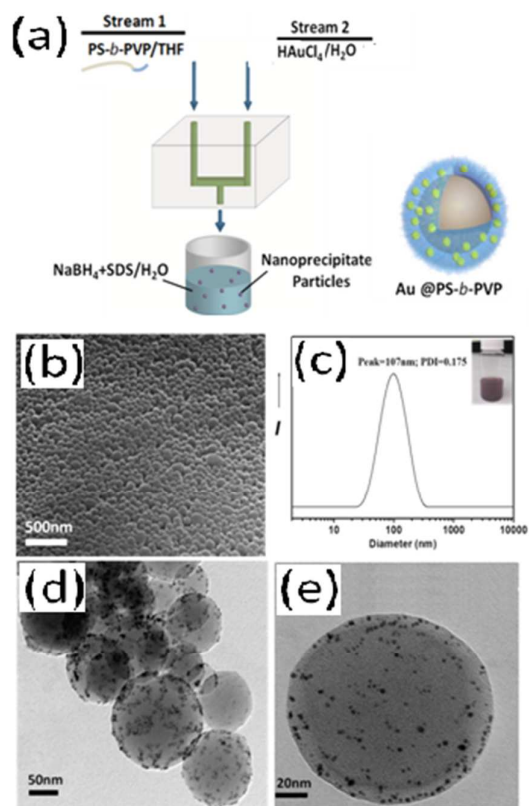
Fig. 14 (a) Schematic process of FNP to produce Au@PS-*b*-PVP, (b)SEM,(b)DLS , (c,d) TEM images of Au@PS-*b*-PVP. Adapted with permission from ref. 125. Copyright 2014, The Royal Society of Chemistry.

non-solvent), with low residence time, continuous process, low energy consumption, and high reproducibility. Priestley and co-workers have used FNP to generate monodisperse polystyrene NPs and illustrated that the sizes of PS NPs can be fine-tuned between 30-150 nm by changing the polymer and/or electrolyte concentration.[118-120] On the other hand, the technique has been successfully used to entrap hydrophobic drug, fluorescent molecules or NPs into biodegradable polymers to make core-shell NPs.[121-124] Using flash nanoprecipitation, Prud'homme and co-workers have demonstrated essentially quantitative incorporation of hydrophobic gold NPs within poly(ε-caprolactone)-block-poly-(ethylene oxide) micelles.[121] The hydrophobic block of the polymer and the hydrophobic NPs are encapsulated in the core. The hydrophilic block forms a corona, sterically stabilizing the particles by preventing further aggregation. Priestley and co-workers recently reported a scalable and continuous preparation route for Au NPs decorated polymer nanosphere core-shell composites through FNP.[125] Fig. 14a shows a schematic FNP process for the formation of polymer@metal NPs composed of two separate streams is used. A syringe containing polystyrene-*b*-poly(*4*-Vinylpyridine) (PS-*b*-PVP) dissolved in THF was placed at the inlet of Stream 1, and a syringe containing HAuCl₄ in H2O was placed at the inlet of Stream 2. Subsequently, fluid was expelled manually from both syringes at the same rate (~1 mL per second), causing the two streams to merge into a mixing stream and then diluted into a

water reservoir containing the reducing agent, NaBH4 and stabilizer, sodium dodecyl sulfate (SDS). The water reservoir quenched the precipitated nanoparticles and a stable colloid solution was obtained (Fig. 14b-e). The process of nanoparticle formation can hence be envisioned as follows: PS-*b*-PVP block polymers self-assemble into NPs with PS as the predominant core and PVP as the corona when the two input streams mix in the confined chamber. Subsequently, $AuCl_4^-$ ions are attracted into the PVP network. The ion-block copolymer complex disperses into a water reservoir containing NaBH₄ that reduces the entrapped $AuCl_4^-$ ions into Au seeds. The growth of gold within the PVP layer then takes place and the complex is quenched to form stable polymer-Au core-shell composites with tunable particle size and gold nanoparticle loading amount by changing the feeding ratio. The reported methodology has also been demonstrated in the successful fabrication of other metal(e.g. Pt, Ag)-polymer nanocomposites.

5. Other methods

Electro-jetting is an attractive way to produce fibers and particles in the industrial scale. Electrospraying and electrospinning designate technologies for fabrication of polymeric nano-/micro-particles and fibers by applying high electrical voltage to polymeric solutions.[126-128] Jeong *et al*. designed a coaxial nozzle in electrspraying setup, where a polymer solution for the core was introduced through the outer nozzle, and the solution for the shell was supplied through the inner nozzle (Fig. 15).[129] When the volumetric feed rate of the shell-forming polycaprolactone (PCL) solution was higher than that of the core forming PS solution, the core-shell structures in uniform size were readily obtained. Electrospinning is essentially an extension of electrospraying process at higher solution concentrations where chain entanglement occurs and is capable of producing polymer fibers at submicron dimensions. The co-electrospinning technique allows one-step fabrication of micro- and nano- core-shell fibers with different pairs of polymers. For instance, Medina-Castillo *et al*. used co-electrospinning of two copolymers to design multifunctional core-shell fibres via a one-step technique: a fluorescent pH-sensitive copolymer was used as the outer fluid, and a suspension formed by polymethyl methacrylate (PMMA) melt magnetic NPs and O₂ indicator was used as the inner fluid.[130] Thus, the core is magnetic and optically sensitive to O₂ while the shell is pH sensitive.

Ultrasonic spray pyrolysis is used to develop a facile one-pot method of synthesizing sandwich structured core-shell particles.[131] During the formation process of a nanoparticle consisting of a Pd core, a V_2O_5 inner layer, and a porous SiO_2 outer layer, PdO was directly reduced to Pd metal in air. Melted V_2O_5 acted as a flux material that accelerated the growth of the Pd crystal. Single-crystalline Pd core particles formed in the center of the composite particles. The amorphous SiO_2 component moved to the outer surface of the particles and formed the outer shell during the formation of crystalline Pd and V_2O_5. V_2O_5 crystals formed the inner shell covering the Pd single-crystal core. The V_2O_5 inner shells were easily washed with distilled water and were dissolved to produce the Pd@SiO_2 yolk-shell structure.
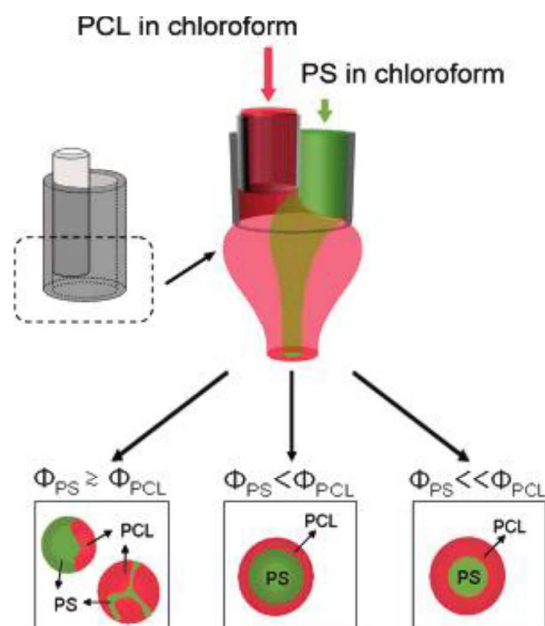
Fig. 15 Schematic illustration of the coaxial electrospraying and possible structures of the colloids consisting of two polymer components. Reproduced with permission from ref. 129. Copyright 2008, American Chemical Society

Direct deposition (e.g. eletrodeposition and chemical vapor deposition) represent another coating technologies for the fabrication of core-shell materials.[132,133] A one-pot synthesis method of PdAu-Au core-shell NPs using electrodeposition and displacement reaction was reported.[132] It was ascertained that Au and Pd atoms were well-distributed inside and Au shell was successfully formed *via* displacement reaction. Ga_2O_3–SnO_2 core–shell microribbon was synthesized *via* a simple one-step chemical vapour deposition from Ga_2O_3–SnO_2–C powder.[133]

6. Conclusion and outlook

We have reviewed the recent progress in the construction of core–shell nanostructures via a one-step/pot strategy. With the rapid development of synthetic chemistry, colloid and interfacial science, and device setup, many core–shell nanostructures have been successfully fabricated via different one-step strategies: e.g., oxidation-reduction, stöber method, self-assembly and employment of different jetting or coating setups. All the methods aim for the green and effective production of core-shell NPs with controllable sizes, composition, architecture and properties though the rational molecular design and materials preparation.

However, though tremendous advances have been made, the one-step/pot strategy in the preparation of core–shell nanostructures is still in its infancy, and many challenges remain to be solved. For example, the facet control of metal@metal or metal@metal oxide crystalline NPs in one-step co-reduction is limited compared to those prepared through two step seed coating process[134]. The current limitation in stöber method is the selection of precursor, mostly now TEOS and phenolic resin based monomer, which would be overcome by other new precursors. Dopamine is a promising candidate. Very recently, Lu and his colleagues found that dopamine could directly polymerize into polydopamine(PDA) nanospheres in a mixture containing water, ethanol, and ammonia at room temperature, similar to stöber condition.[135] In addition, PDA has been shown to be an effective carbon source for the

formation of carbon-coated materials.[136,137] Compared to the carbon spheres obtained by carbonization of phenol/formaldehyde resins, the PDA-derived carbon spheres contained nearly 100% of sp^2C (graphitic carbon) and high-level electroactive nitrogen species, thus exhibiting enhanced electroconductivity.[138-140] Therefore, the application of dopamine in the one-step stöber preparation of core-shell NPs would expand the new synthesis pathway as well as endow more new functions.

The bottleneck in self-assembly methodologies is to find an efficient, feasible, low cost, and easy way to scale up for designing various functional core-shell polymer NPs. The versatility and low productivity of both co-precipitation and microfluidic approaches have limited their application for industrial production. FNP has many distinctive advantages, which render it a transformative route for commercial nanocolloid production: i) one-step and continuous process, ii) room temperature and low energy process, and iii) proven scalability. A variety of polymers can be employed in FNP as well as facilitate the simultaneous entrapment of various functional (e.g., magnetic, fluorescent) cores during the precipitation process. The strategy is therefore a simple and versatile synthetic approach towards designing multifunctional and novel nanostructures for different applications. For example, Janus-based core-shell nanocomposites would be formed when inducing the phase separation of dissimilar polymers in nano-domains precipitated during FNP. An indispensable feature of FNP is that key process parameters and molecular features of the polymers can be independently manipulated for the facile control particle size, composition and surface chemistry. It is worthy to note that the FNP mixers are not microfluidics devices. Microfluidics geometries are intrinsically poor mixers, even with the incorporation of mixing elements, because they operate at low Reynolds numbers. All of the fluid streams in FNP mixers experience the high energy mixing (Reynolds numbers > 1000), resulting in the achievement of uniform supersaturations as high as 10,000 in 1.5 ms.[141] This drives the high nucleation rates that enable high concentration processing of nanoparticles and production capacity. Using continuous flow in the current geometry would enable production of 3.5 kg/day of material, and currently commercial production of *b*-carotene NPs are produced at 1400 kg/day using confined impinging jet technology.

Along with the development of materials science, chemistry and fluid mechanics, core-shell nanomaterials and other nanocomposite could be efficiently designed and fabricated with experimentally controllable size, composition and chemical ordering under suitable reaction conditions, choice of precursors, and combination physical, chemical, and biological generation methods. The one-step or one-pot strategies presented this review are expected to provide a simple and versatile synthetic approach towards designing multifunctional assemblies and other novel nanostructures for biological, energy, and environmental applications.

Acknowledgements

Notes and references

1. R. G. Chaudhuri and S. Paria, *Chem. Rev.*, 2012, **112**, 2373.
2. R. Hayes, A. Ahmed, T. Edge and H. Zhang, *J. Chromatogr. A*, 2014, **1357**, 36.
3. Q. Sun, X.-Q. Zhang, Y. Wang and A.-H. Lu, *Chin. J. Catal.*, 2015, **36**, 683.
4. M. B. Gawande, A. Goswami, T. Asefa, H. Guo, A. V. Biradar , D. Peng, R. Zboril and R. S. Varma, *Chem. Soc. Rev.,* 2015, **44**, 7540
5. G. Li and Z. Tang, *Nanoscale*, 2014, **6**, 3995.
6. X. L. Zhang, H. Y. Niu, W. H. Li, Y. L. Shi and Y. Q. Cai, *Chem. Commun.*, 2011, **47**, 4454.
7. J. Liu, S. Z. Qiao, J. S. Chen, X. W. Lou, X. Xing and G. Q. Lu, *Chem. Commun.,* 2011, **47**, 12578.
8. H. H. Park, K. Woo and J. P. Ahn, *Sci. Rep.*, 2013, **3**, 1497.
9. X. Lai, J. Li, B. A. Korgel, Z. Dong, Z. Li, F. Su, J. Du and D. Wang, *Angew. Chem. Int. Ed.*, 2011, **50**, 2738.
10. R. Gui, A. Wan and H. Jin, *Analyst*, 2013, **138**, 5956.
11. T. Li, J. Moon, A. A Morrone, J. J. Mecholsky, D. R. Talham and J. H. Adair, *Langmuir*, 1999, **15**, 4328.
12. S. Balakrishnan, M. J. Bonder and G. C. Hadjipanayis, *J. Magn. Magn. Mater.*, 2009, **321**, 117.
13. R. A. Caruso, A. Susha and F. Caruso, *Chem. Mater.*, 2001, **13**, 400.
14. S. Shi, Y. Yu, T. Wang, Q. Wang, C. Wang, S. Kuroda, *Chin. J. Polym. Sci.,* 2014, **32**, 524.
15. J. Hu, M. Chen, X. Fang and L. Wu, *Chem. Soc. Rev.*, 2011, **40**, 5472.
16. X. Lai, J. E. Halpert and D. Wang, Energy Environ. Sci., 2012, **5**, 5604.
17. X. Liu, J. Yang, L. Zha and Z. Jiang, *Chin. J. Polym. Sci.,* 2014, **32**, 1544.
18. W. Tong, X. Song and C. Gao, *Chem. Soc. Rev.*, 2012, **41**, 6103.
19. J. Moraes, K. Ohno, T. Maschmeyer and S. Perrier, *Chem. Mater.,* 2013, **25**, 3522.
20. G. L. Li, H. Mohwald and D. G. Shchukin, *Chem. Soc. Rev.*, 2013, **42**, 3628.
21. R. A. Perez and H. W. Kim, *Acta Biomater.*, 2015, **21**, 2.
22. D. Vasudevan, R. R. Gaddam, A. Trinchi and I. Cole, *J. Alloys Comp.,* 2015, **636**, 395.
23. A. Mirzaei, K. Janghorban, B. Hashemi and G. Neri, *J. Nanopart. Res.*, 2015, **17**,371.
24. J.-M. Yan, X.-B. Zhang, T. Akita, M. Haruta and Q. Xu, *J. Am. Chem. Soc.*, 2010, **132**, 5326.
25. K. Aranishi, H.-L. Jiang, T. Akita, M. Haruta and Q. Xu, *Nano Res.*, 2011, **4**, 1233.
26. S. Kang, Y. W. Lee, Y. Park, B. S. Choi, J. W. Hong, K. H. Park and S. W. Han, *ACS Nano*, 2013, **7**, 7945.
27. Y. W. Lee, M. Kim, Z. H. Kim and S. W. Han, *J. Am. Chem. Soc.*, 2009, **131**, 17036
28. X. Huang, H. Wu, S. Pu, W. Zhang, X. Liao and B. Shi, *Green Chem.*, 2011, **13**, 950.
29. Z.-L. Wang, J.-M. Yan, H.-L. Wang, Y. Ping and Q. Jiang, *J. Mater. Chem. A,* 2013, **1**, 12721.
30. L. Kuai, X. Yu, S. Wang, Y. Sang and B. Geng, *Langmuir*, 2012, **28**, 7168.
31. R. Harpeness and A. Gedanken *Langmuir*, 2004, **20**, 3431.
32. Y. Xu, Y. Dong, J. Shi, M. Xu, Z. Zhang and X. Yang, *Catal. Commun.*, 2011, **13**, 54.
33. L. Wang and Y. Yamauchi, J. *Am. Chem. Soc.,* 2010, 132, 13636.
34. L. Xia, X. Hu, X. Kang, H. Zhao, M. Sun and X. Cihen, *Colloids Surf., A,,* 2010, **367**, 96.
35. J. Guo, X. Wang, P. Miao, X. Liao, W. Zhang and B. Shi, *J. Mater. Chem.,* 2012, **22**, 11933.
36. S. Anandan, F. Grieser and M. Ashokkumar, *J. Phys. Chem. C*, 2008, **112**, 15102
37. H. Zhang, J. Okuni and N. Toshima, *J. Colloid Interface Sci.,* 2011, **354**, 131.
38. H. Zhang, Y. J. Yin, Y. J. Hu, C. Y. Li, P. Wu, S. H. Wei and C. X. Cai, *J. Phys. Chem. C*, 2010, **114**, 11861
39. Y. Kim, Y. W. Lee, M. Kim and S. W. Han, *Chem. Eur. J.,* 2014, **20**, 7901.
40. Y. Kim, Y. Noh, E. J. Lim, S. Lee, S. M. Choi and W. B. Kim, *J. Mater. Chem. A*, 2014, **2**, 6976.
41. H.-L. Wang, J.-M. Yan, Z.-L. Wang and Q. Jiang, Int. J. Hydrogen Energy*,* 2012, **37**, 10229.
42. Z. Xiong, L. Zhang and X. S. Zhao, *Chem. Eur. J.*, 2014, **20**, 14715.
43. T. Mitsudome, Y. Mikami, M. Matoba, T. Mizugaki, K. Jitsukawa and K. Kaneda, *Angew. Chem. Int. Ed.*, 2012, **51**, 136.
44. T. Kayama, K. Yamazaki and H. Shinjoh, *J. Am. Chem. Soc.*, 2010, **132**, 13154
45. X. Wang, D. Liu, S. Song and H. Zhang, *J. Am. Chem. Soc.*, 2013, **135**, 15864.
46. S. Song, X. Wang and H. Zhang, *NPG Asia Mater.*, 2015, **7**, e179.
47. D. Muñoz-Rojas, J. Oró-Solé, O. Ayyad and P. Gómez-Romero, *J. Mater. Chem.,* 2011, **21**, 2078.
48. D. Munoz-Rojas, J. Oro-Sole, O. Ayyad and P. Gomez-Romero, *Small*, 2008, **4**, 1301.
49. W. Hu, H. Chen and C. M. Li, *Colloid Polym. Sci.,* 2014, **293**, 505.
50. L. Gao, S. Lv and S. Xing, *Synth. Met.*, 2012, **162**, 948.
51. M. R. Karim, K. T. Lim, C. J. Lee, M. T. I. Bhuiyan, H. J. Kim, L.-S. Park and M. S. Lee, *J. Polym. Sci. Part A: Polym. Chem.,* 2007, 45, 5741-5747.
52. B. Zhao and Z. Nan, *Mater. Sci. Eng.: C*, 2012, **32**, 1971.
53. A. J. Suryawanshi, P. Thuptimdang, J. Byrom, E. Khan and V. J. Gelling, *Synth. Met.,* 2014, **197**, 134.
54. Z. Wang, J. Yuan, D. Han, L. Niu and A. Ivaska, *Nanotechnology*, 2007, **18**, 115610.
55. J. Suárez-Guevara, O. Ayyad and P. Gómez-Romero, *Nanoscale Res. Lett.,* 2012, **7**, 1
56. H. Lee*,* S. H. Dellatore*,* W. M. Miller and P. H. Messersmith*, Science,* 2007*,* **318***,* 426.
57. J.-J. Feng, P.-P. Zhang, A.-J. Wang, Q.-C. Liao, J.-L. Xi and J.-R. Chen, *New J. Chem.*, 2012, **36**, 148.
58. E. Mazario, J. Sanchez-Marcos, N. Menendez, P. Herrasti, M. Garcia-Hernandez and A. Munoz-Bonilla, *RSC Adv.,* 2014, **4**, 48353
59. C. M. Cui, X. H. Guo, Y. M. Geng, T. T. Dang, G. Xie, S. P. Chena and F. Q. Zhao, *Chem. Commun.*, 2015, **51**, 9276.
60. H. Qiao, L. Xiao, Z. Zheng, H. Liu, F. Jia and L. Zhang, *J. Power Sources*, 2008, **185**, 486.
61. Y. Cheng, X. Niu, T. Zhao, F. Yuan, Y. Zhu and H. Fu, *Eur. J. Inorg. Chem.,* 2013, 4988.
62. I. Pastoriza-Santos*,* D. S. Koktysh*,* A. Mamedow*,* M. Giersig*,* N. A. Kotov*,* L. M. Liz-Marzán*, Langmuir* 2000*,* **16***,* 27.
63. J. Zheng, Z. Q. Liu, X. S. Zhao, M. Liu, X. Liu and W. Chu, *Nanotechnology*, 2012, **23**, 165601.
64. W. Kang, H. Li, Y. Yan, P. Xiao, L. Zhu, K. Tang, Y. Zhu and Y. Qian, *J. Phys. Chem. C*, 2011, **115**, 6250.
65. J. C. Yu, X. Hu, Q. Li, Z. Zheng and Y. Xu, *Chem. Eur. J.*, 2005, **12**, 548.
66. R. Yang, W. Zhao, J. Zheng, X. Zhang and X. Li, J. Phys. Chem. C, 2010, **114**, 20272.
67. X. W. Lou, J. S. Chen, P. Chen and L. A. Archer, *Chem. Mater.,* 2009, **21**, 2868.
68. W. Wang, G. Ding, T. Jiang, P. Zhang, T. Wu and B. Han, *Green Chem.,* 2013, **15**, 1150.
69. X. Sun and Y. Li, *Langmuir* 2005**, 21**, 6019.
70. X. Sun and Y. Li, *Angew. Chem. Int. Ed.,* 2004, **43**, 597.
71. X. Sun, J. Liu and Y. Li, *Chem. Mater.* 2006*,* **18**, 3486.

72. G. B. Yu , B. Sun , Y. Pei , S. H. Xie , S. R. Yan , M. H. Qiao , K. N. Fan , X. X. Zhang and B. N. Zong , *J. Am. Chem. Soc.* 2010 , **132** , 935

73. Z. Wang, J. S. Chen, T. Zhu, S. Madhavi and X. W. Lou, *Chem Commun.*, 2010, **46**, 6906.

74. W. Stöber, A. Fink, E. Bohn, *J. Colloid Interface Sci.* 1968, **26**, 62

75. J. Chen, R. Zhang, L. Han, B. Tu and D. Zhao, *Nano Res.,* 2013, **6**, 871.

76. R. Veneziano, G. Derrien, S. Tan, A. Brisson, J. M. Devoisselle, J. Chopineau and C. Charnay, *Small,* 2012, **8**, 3674.

77. L. Wang, T.-Y. Cheang, S. Wang, Z. Hu, Z. Xing, W. Qu and A. Xu, *J. Mater. Res.,* 2012, **27**, 2425.

78. L. Han, H. Wei, B. Tu and D. Zhao, *Chem. Commun.*, 2011, **47**, 8536.

79. Y. Li, Z. Jin, T. Li and Z. Xiu, The Science of the total environment, 2012, 421-422, 260-266.

80. Q. Yao, Z. H. Lu, Z. Zhang, X. Chen and Y. Lan, *Sci. Rep.,* 2014, **4**, 7597.

81. X. Du, L. Yao and J. He, *Chem. Eur. J.*, 2012, **18**, 7878.

82. M. E. Aguirre, H. B. Rodríguez, E. San Román, A. Feldhoff and M. A. Grela, *J. Phys. Chem. C,* 2011, **115**, 24967.

83. .

84. S. W. Jun, M. Shokouhimehr, D. J. Lee, Y. Jang, J. Park and T. Hyeon, *Chem. Commun.,* 2013, **49**, 7821.

85. A. Ahmed, H. Ritchie, P. Myers and H. Zhang, *Adv. Mater.,* 2012, **24**, 6042.

86. A. Ahmed, W. Abdelmagid, H. Ritchie, P. Myers and H. Zhang, *J. Chromatogr. A,* 2012, **1270**, 194.

87. J. Liu, S. Z. Qiao, H. Liu, J. Chen, A. Orpe, D. Y. Zhao and G. Q. M. Lu, *Angew. Chem., Int. Ed.*, 2011, **50**, 5947

88. A. B. Fuertes, P. Valle-Vigon and M. Sevilla, *Chem. Commun.*, 2012, **48**, 6124.

89. T. Yang, J. Liu, Y. Zheng, M. J. Monteiro and S. Z. Qiao, *Chem. Eur. J.,* 2013, 19, 6942.

90. H. Qian, E. Zhu, S. Zheng, Z. Li, Y. Hu, C. Guo, X. Yang, L. Li, G. Tong and H. Guo, *Nanotechnology*, 2010, 21, 495602.

91. M. Kim, K. Sohn, H. B. Na, T. Hyeon, *Nano Lett.*, 2002, 2, 1383.

92. A. B. Fuertes, M. Sevilla, T. Valdes-Solis, P. Tartaj, *Chem. Mater.,* 2007, 19, 5418

93. J. X. Zhu, T. Sun, H. H. Hng, J. Ma, F. Y. C. Boey, X. W. Lou, H. Zhang, C. Xue, H. Y. Chen, Q. Y. Yan, *Chem. Mater.*, 2009, **21**, 3848.

94. R. Liu, F. Qu, Y. Guo, N. Yao and R. D. Priestley, *Chem. Commun.*, 2014, **50**, 478.

95. C. Jin, Y. Wang, H. Tang, H. Wei, X. Liu and J. Wang, *J. Phys. Chem. C*, 2014, **118**, 25110.

96. R. Liu, Y. Yeh, V. Tam, F. Qu, N. Yao and R. D. Priestley, *Chem. Commun.*, 2014, **50**, 9056

97. B.-S. Kim, J. M. Qiu, J. P. Wang, T. A. Taton, *Nano Lett.* 2005, **5**, 1987.

98. Y. Kang and T. A. Taton, *Angew. Chem. Int. Ed.,* 2005, **44**, 409.

99. Y. Chen, J. Cho, A.Young and T. A. Taton, *Langmuir* 2007, **23**, 7491.

100. A. Pavia-Sanders, S. Zhang, J. A. Flores, J. E. Sanders, J. E. Raymond and K. L. Wooley, *ACS Nano*, 2013, **7**, 7552.

101. Q. Luo, R. J. Hickey and S.-J. Park, *ACS Macro Lett.*, 2013, **2**,

102. R. J. Hickey, A. S. Haynes, J. M. Kikkawa and S. J. Park, *J. Am. Chem. Soc.,* 2011, 133, 1517

103. H. Yabu, K. Koike, K. Motoyoshi, T. Higuchi and M. Shimomura, *Macro. Rapid commun.,* 2010, **31**, 1267.

104. A. Abou-Hassan, O. Sandre and V. Cabuil, *Angew. Chem. Int. Ed.*, 2010, **49**, 6268.

105. S. Marre and K. F. Jensen, *Chem. Soc. Rev.*, 2010, **39**, 1183.

106. W. Wang, M. J. Zhang and L. Y. Chu, *Acc. Chem. Res.*, 2014,

107. W. Wang, M. J. Zhang and L. Y. Chu, *Curr. Opin. Pharmacol.*, 2014, 18, 35-41.

108. W. Lan, S. Li, J. Xu and G. Luo, *Langmuir*, 2011, **27**, 13242.

109. J. Wu, T. Kong, K. W. Yeung, H. C. Shum, K. M. Cheung, L. Wang and M. K. To, *Acta Biomater.,* 2013, **9**, 7410.

110. T. T. Kong, J. Wu, K. W. K. Yeung, M. K. T. To, H. C. Shum and L. Q. Wang, *Biomicrofluidics*, 2013, **7**, 044128.

111. G. Schabas, H. Yusuf, M. G. Moffitt and D. Sinton, *Langmuir*, 2008, **24**, 637.

112. P. M. Valencia, P. A. Basto, L. F. Zhang, M. Rhee, R. Langer, O. C. Farokhzad and R. Karnik, *ACS Nano*, 2010, **4**, 1671.

113. R. Karnik, F. Gu, P. Basto, C. Cannizzaro, L. Dean, W. Kyei-Manu, R. Langer and O. C. Farokhzad, *Nano Lett.* 2008, **8**, 2906.

114. B. K. Johnson, R. K. Prud'homme, *AIChE J.* 2003, 49, 2264.

115. B. K. Johnson, R. K. Prud'homme, *Phys. Rev. Lett.* 2003, 91;

116. B. K. Johnson, R. K. Prud'homme, *Aust. J. Chem.* 2003, 56, 1021.

117. K M. Pustulka, A. R. Wohl, H. S. Lee, A. R. Michel, J. Han, T. R. Hoye, A. V. McCormick, J. Panyam, C. W. Macosko, *Mol. Pharmaceutics*, 2013, 10, 4367

118. C. Zhang, V. J. Pansare, R. K. Prud'homme, R. D. Priestley, *Soft Matter*, 2012, 8, 86

119. J.W. Chung, K. Lee, C. Neikirk, C. Nelson, R.D. Priestley, *Small*, 2012, 8, 1693;

120. J. W. Chung, C. Neikirk, R.D. Priestley, *J. Colloid Interface Sci.*, 2013, **396**, 16.

121. M. E. Gindy, A. Z. Panagiotopoulos and R. K. Prud'homme, *Langmuir* 2008, **24**, 83.

122. J. Shan, S. J. Budijono, G. Hu, N. Yao, Y. kang, Y. Ju and R. K. Prud'homme, *Adv. Funct. Mater.*, 2011, **21**, 2488.

123. V. Kumar, D. H. Adamson and R. K. Prud'homme, *Small*, 2010, **6**, 2907.

124. N. M. Pinkerton, S. W. Zhang, R. L. Youngblood, D. Gao, S. Li, B. R. Benson, J. Anthony, H. A. Stone, P. J. Sinko and R. K. Prud'homme, *Biomacromolecules,* 2014, **15**, 252.

125. R. Liu, C. Sosa, Y.-W. Yeh, F. Qu, N. Yao, R. K. Prud'homme and R. D. Priestley, *J. Mater. Chem. A*, 2014, **2**, 17.

126. C. L. Zhang and S. H. Yu, *Chem. Soc. Rev.*, 2014, **43**, 4423.

127. A. Greiner and J. H. Wendorff, *Angew. Chem. Int. Ed.*, 2007, **46**, 5670.

128. Y. Wu, I. C. Liao, S. J. Kennedy, J. Du, J. Wang, K. W. Leong and R. L. Clark, *Chem. Commun.*, 2010, **46**, 4743.

131. Y. N. Ko, Y. C. Kang and S. B. Park, *Chem. Commun.*, 2013, **49**, 3884

132. A. L. Medina-Castillo, J. F. Fernández-Sánchez and A. Fernández-Gutiérrez, *Adv. Funct. Mater.,* 2011, **21**, 3488.

133. Y. N. Ko, Y. C. Kang and S. B. Park, *Chem. Commun.*, 2013, **49**, 3884

134. M. H. Huang and P. H. Lin, *Adv. Funct. Mater.*, 2012, **22**, 14.

135. M. J. Kim, K. J. Park, T. Lim, S. Choe, T. Yu and J. J. Kim, *J. Electrochem. Soc.,* 2012, **160**, E1.

136. K. Liu, M. Sakurai and M. Aono, J. *Mater. Chem.,* 2012, **22**, 12882.

137. K. Ai, Y. Liu, C. Ruan, L. Lu and G. M. Lu, *Adv. Mater.,* 2013, **25**, 998.

138. N. Liu, H. Wu, M. T. McDowell, Y. Yao, C. Wang and Y. Cui, *Nano Lett.,* 2012, **12**, 3315.

139. C. Lei, F. Han, D. Li, W. C. Li, Q. Sun, X. Q. Zhang and A. H. Lu, *Nanoscale*, 2013, **5**, 1168.

140. J. Kong, W. A. Yee, L. Yang, Y. Wei, S. L. Phua, H. G. Ong, J. M. Ang, X. Li and X. Lu, *Chem. Commun.*, 2012, **48**, 10316.

141. S. M. D'Addio and R. K. Prud'homme, *Adv. Drug Deliv. Rev.*, 2011, **63**, 417.

Rui Liu received his PhD in chemistry from University of California, Riverside in 2010. He carried out his first postdoctoral research at Oak Ridge National Laboratory. In 2012-2015, he was a postdoctoral associate in the laboratory of Professor Rodney Priestley at Princeton University. In 2015, he joined Tongji University as a Young Thousand Talented professor. His research interests include nanoparticle preparation and polymer self-assembly.

Rodney D. Priestley is an Associate Professor in the Department of Chemical and Biological Engineering at Princeton University. He obtained his Ph.D. in Chemical Engineering from Northwestern University in 2008. He completed a NSF/Chateaubriand postdoctoral fellowship at Ecole Superieure de Physique et Chimie Industrielles de la Ville de Paris. His research interests include polymer glasses, nanoconfined polymer dynamics, polymer thin film and nanoparticle formation, MAPLE and responsive polymers. He is the recipient of numerous awards including the Quadrant Award, ACS New Investigator Grant, 3M Non-Tenured Faculty Grant, NSF CAREER Award, AFOSR YIP, Presidential Early Career Award for Scientist and Engineers, Alfred P. Sloan Fellowship and Camille Dreyfus Teacher-Scholar Award. Most recently he was named to The Root 100 list of most influential African American in 2014.